Redox Biology 29 (2020) 101406

Contents lists available at ScienceDirect

Redox Biology

journal homepage: www.elsevier.com/locate/redox

# Noise-induced loss of sensory hair cells is mediated by ROS/AMPKα pathway

Fan Wu[a,b,1], Hao Xiong[a,b,1], Suhua Sha[a,*]

[a] Department of Pathology and Laboratory Medicine, Medical University of South Carolina, Charleston, SC, 29425, USA
[b] Department of Otolaryngology, Sun Yat-sen Memorial Hospital, Sun Yat-sen University, Guangzhou, China

ARTICLE INFO

*Keywords:*
Noise-induced hearing loss
Activation of AMPKα
Reactive oxygen species
Forskolin
4-Hydroxynonenal
3-Nitrotyrosine
N-acetyl cysteine
Sensory hair cells

ABSTRACT

The formation of reactive oxygen species (ROS) is a well-documented process in noise-induced hearing loss (NIHL). We have also previously shown that activation of 5' adenosine monophosphate (AMP)-activated protein kinase (AMPKα) at its catalytic residue T172 is one of the key reactions triggering noise-induced outer hair cell (OHC) death. In this study, we are addressing the link between ROS formation and activation of AMPKα in OHCs after noise exposure. *In-vivo* treatment of CBA/J mice with the antioxidant N-acetyl cysteine (NAC) reduced noise-induced ROS formation (as assessed by the relative levels of 4-hydroxynonenal and 3-nitrotyrosine) and activation of AMPKα in OHCs. Forskolin, an activator of adenylyl cyclase (AC) and an antioxidant, significantly increased cyclic adenosine monophosphate (cAMP) and decreased ROS formation and noise-induced activation of AMPKα. Consequently, treatment with forskolin attenuated noise-induced losses of OHCs and NIHL. In HEI-OC1 cells, $H_2O_2$-induced activation of AMPKα and cell death were inhibited by the application of forskolin. The sum of our data indicates that noise activates AMPKα in OHCs through formation of ROS and that noise-exposure-induced OHC death is mediated by a ROS/AMPKα-dependent pathway. Forskolin may serve as a potential compound for prevention of NIHL.

## 1. Introduction

A main causative factor in noise-induced hearing loss (NIHL) is oxidative stress, inflicting damage on sensory hair cells [1]. In fact, the appearance of ROS and their oxidative products such as 4-hydroxynonenal (4-HNE) and 3-nitrotyrosine (3-NT) in cochlear tissues has been well documented as a general pathologic mechanism of different inner ear insults, including administration of ototoxic drugs, excessive noise exposure, and the aging process [2–6]. Conversely, the antioxidant defense system is activated as a protective reaction to potential inner ear insults [7]. Importantly, evidence for causal relationship between oxidative damage and hearing loss is supported by the fact that antioxidant treatment reduces sensory hair cell death triggered by aminoglycoside antibiotics [8–10] or noise exposure [11,12].

Recently, we found that noise exposure activates 5' adenosine monophosphate (AMP)-activated protein kinase alpha subunits (AMPKα) and that blockade of such activation by small interfering RNA (siRNA) or the specific inhibitor compound C effectively reduced noise-induced auditory hair cell death and NIHL [13]. Inhibition of upstream kinases to AMPKα such as liver kinase B1 (LKB1) also protected from noise-induced damage [13]. AMPK is an essential cellular energy sensor activated by various types of metabolic stress, drugs, and xenobiotics [14]. AMPK is mainly activated in an AMP/ATP-ratio-dependent fashion, but it also activated in an AMP/ATP-independent fashion [15,16]. Increased intracellular levels of AMP and ADP, which result from a reduction of ATP, activate AMPKα through increased binding of AMP or ADP to the AMPK γ-subunit. AMPK can also be activated by phosphorylation of Thr-172 (p-AMPKα T172) via LKB1 or by inhibition of Thr-172 dephosphorylation [15,17–21]. Although changes in AMP levels remain the principal activator of AMPK, pro-oxidants, such as NO and peroxynitrite, can trigger the metabolic gatekeeper, AMPK. The activation of AMPK by ROS has been widely speculated and discussed [14,22–24]. Under hypoxic conditions, activation of AMPK is elicited in a ROS-dependent manner, leading to apoptotic cell death [25]. Additionally, AMPK can be activated by oxidative stress [14,22–24,26–28] possibly through the reversible oxidation of cysteine residues at the AMPKα subunit [27]. We hypothesize that oxidative stress associated with noise exposure activates AMPKα in OHCs. Furthermore, while

* Corresponding author. Department of Pathology and Laboratory Medicine, Medical University of South Carolina, Walton Research Building, Room 403-E, 39 Sabin Street, Charleston, SC, 29425, USA.
*E-mail address:* shasu@musc.edu (S. Sha).
[1] Fan Wu and Hao Xiong had equal contributions to this project.

https://doi.org/10.1016/j.redox.2019.101406
Received 30 October 2019; Received in revised form 25 November 2019; Accepted 9 December 2019
Available online 14 December 2019

**Abbreviations:**

| | |
|---|---|
| 3-NT | 3-nitrotyrosine |
| 4-HNE | 4-hydroxynonenal |
| ABR | Auditory brainstem response |
| AC | Adenylyl cyclase |
| AMPKα | 5′ adenosine monophosphate-activated protein kinase (AMPKα) |
| cAMP | Cyclic adenosine monophosphate |
| CCK-8 | Cell counting kit |
| CREB | cAMP response binding element |
| DMSO | Dimethyl sulfoxide |
| FSK | Forskolin |
| IHC | Inner hair cell |
| IP | Intraperitoneal |
| LKB1 | Liver kinase B1 |
| NAC | N-acetyl cysteine |
| NaOH | Sodium hydroxide |
| NIHL | Noise-induced hearing loss |
| OHC | Outer hair cell |
| PBS | Phosphate buffered saline |
| PBS-T | PBS with 0.1% Tween 20 |
| PKA | Protein kinase A |
| PTS | Permanent threshold shifts |
| ROS | Reactive oxygen species |
| SDS-PAGE | Sodium dodecyl sulfate polyacrylamide gel electrophoresis |
| SPL | Sound pressure level |
| TDT | Tucker Davis Technology |
| TTS | Temporary threshold shifts |
| VGCC | Voltage-gated calcium channels |
| FBS | Fetal bovine serum |
| FITC | Fluorescein isothiocyanate |
| OBN | octave band noise |
| PI | Propidium iodide |
| RIPA | Radio-immunoprecipitation assay |

ROS can act as positive regulators of AMPK activity, antioxidants negatively regulate AMPK activation [22,23]. Hence, antioxidants that attenuate NIHL should also prevent the activation of AMPK.

Forskolin, an activator of adenylate cyclase [29], has been used as an effective treatment for a wide range of diseases, including hypertension, asthma, diabetes mellitus, and heart disease [30]. Forskolin has also shown antioxidant effects in several studies [31–33]. As a case in point, treatment with forskolin attenuates drug ototoxicity by inhibiting ROS production [34]. Based on the pharmacological characteristics of forskolin and the pathology of NIHL, we hypothesize that forskolin can prevent NIHL. In this study, we manipulated ROS formation using NAC and forskolin to evaluate AMPK activation in OHCs after noise exposure. We then assessed the auditory function of adult male CBA/J mice with or without forskolin treatment under noise conditions that induce permanent auditory threshold shifts (PTS) with losses of outer and inner hair cells. Finally, we tested activation of AMPKα by administration of $H_2O_2$ to an inner ear cell line (HEI-OC1) and the effect of forskolin against $H_2O_2$-induced cell death in order to probe the relationship between ROS formation and activation of AMPK.

## 2. Materials and methods

### 2.1. Animals

Male CBA/J mice at 6 weeks of age were purchased from The Jackson Laboratory. All mice had free access to water and a regular mouse diet (Irradiated Lab Diet #5V75) and were kept at 22 ± 1 °C under a standard 12:12 h light-dark cycle to acclimate for at least 1 week before conducting baseline auditory brainstem response (ABR) measurements. All mice were housed in the animal facility of the Children's Research Institute at the Medical University of South Carolina. All research protocols were approved by the Institutional Animal Care and Use Committee at MUSC. Animal care was under the supervision of the Division of Laboratory Animal Resources at MUSC. Table 1 illustrates general experimental timeline.

### 2.2. Noise exposure

In this study, unrestrained male CBA/J male mice at the age of 8 weeks (one mouse per stainless steel wire cage, approximately 9 $cm^3$) were exposed to octave band noise (OBN) with a frequency spectrum from 8–16 kHz at 100 dB sound pressure level (SPL) for 2 h to induce

**Table 1**
CBA/J mice from Jackson laboratory arrived at MUSC at the age of 6 weeks. Baseline auditory brainstem responses (ABRs) were measured at the age of 7 weeks. At the age of 8 weeks, mice were exposed to octave band noise (OBN) at 100 dB for 2 h. Two weeks after the noise exposure (10 weeks), mice were euthanized for surface preparations for hair cell counts (left ear) and ribbon counts (right ear) after final ABR measurements. For immunohistochemistry, mice were euthanized 1 h or 24 h after the completion of noise exposure. For the experiments to evaluate molecular signaling by immunolabeling, pharmaceutical compounds NAC and forskolin were injected via intraperitoneal (IP) route 24 h and 1 h before, and immediately after the noise exposure. For experiments to observe the progress of auditory threshold shifts, mice received one additional IP injection of the pharmaceutical compounds.

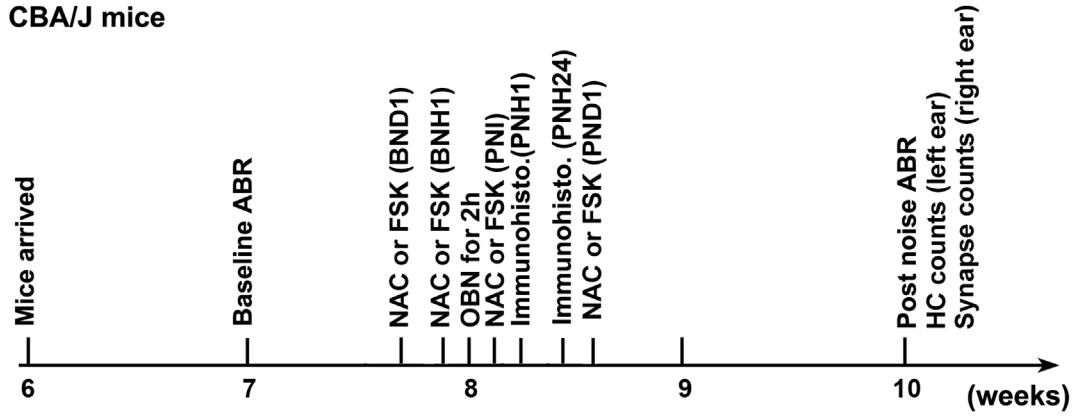

permanent threshold shifts with loss of IHC synaptic ribbons and sensory hair cells including OHCs and IHCs by 14 d after the noise exposure. The sound exposure chamber was fitted with a loudspeaker (model 2450H; JBL) driven by a power amplifier (model XLS 202D; Crown Audio) fed from a CD player (model CD-200; Tascam TEAC American). Audio CD sound files were created and equalized with audio editing software (Audition 3; Adobe Systems, Inc.). The background sound intensity of the environment surrounding the cages was 65 dB as measured with a sound level meter (model 1200; Quest Technologies). Sound levels for noise exposure were measured with a sound level meter at multiple locations within the sound chamber to ensure the uniformity of the sound field and measured before and after exposure to ensure stability. Control mice were kept in silence (without use of the loudspeaker) within the same chamber for 2 h.

### 2.3. Drug administration via intra-peritoneal route

Both forskolin (#F3917) and NAC (# A7250) were purchased from Sigma-Aldrich. Forskolin was dissolved in dimethyl sulfoxide (DMSO) as stock solution (100 mM) and stored at - 20 °C, as previously described [35]. The stock solution was diluted with 0.9% saline solution immediately before injections. Initially, we tested two doses of forskolin (5 mg/kg and 10 mg/kg) for prevention of NIHL. Since 5 mg/kg of forskolin attenuated NIHL, we used 5 mg/kg for the rest of the experiments. NAC was dissolved in 0.2 M sodium hydroxide (NaOH) as a stock solution (130 mg/ml) and stored at -20 °C. The final NAC solution was adjusted to pH 7.0 before being injected into animals. For immunohistochemistry, each animal received a total of three intraperitoneal (IP) injections of forskolin at a dose of 5 mg/kg per injection or NAC at a dose of 325 mg/kg based on conditions reported in our previous study [36]. Vehicle control mice received the same volume of DMSO or saline. Three IP injections were administered 24 h before, 2 h before, and immediately after noise exposure. The mice used for experiments to observe the progression of ABR thresholds received one additional IP injection on the following day, which is 24 h post noise exposure.

### 2.4. Auditory brainstem response measurements

ABRs were measured in the left ears of anaesthetized mice before and two weeks after noise exposure. Mice were anesthetized with an IP injection of a mixture of ketamine (100 mg/kg) and xylazine (10 mg/kg), and then placed in a sound-isolated and electrically shielded booth (Acoustic Systems). Body temperature was monitored and maintained near 37 °C with a heating pad. Acoustic stimuli were delivered monaurally to a Beyer earphone attached to a customized plastic speculum inserted into the ear canal. Subdermal electrodes were inserted at the vertex of the skull (active), mastoid region under the left ear, and mastoid region under the right ear (ground). ABRs were measured at 8, 16, and 32 kHz. Tucker Davis Technology (TDT) System III hardware and SigGen/Biosig software were used to present the stimuli (15 ms duration tone bursts with 1 ms rise-fall time) and record the response. Up to 1024 responses were averaged for each stimulus level. ABR wave I was used to determine ABR thresholds for each frequency. Thresholds were determined for each frequency by reducing the intensity in 10-dB increments and then in 5-dB steps near threshold until no organized responses were detected. Thresholds were estimated between the lowest stimulus level where a response was observed and the highest level without response. All ABR measurements were conducted by the same experimenter. The ABR values were assigned by an expert who was blinded to the treatment conditions.

### 2.5. Immunocytochemistry for cochlear surface preparations

The temporal bones were removed and perfused locally with a solution of 4% paraformaldehyde in PBS, pH 7.4, and kept in this fixative overnight at 4 °C. For immunolabeling of IHC synapses, the cochleae were perfused locally with a solution of 4% paraformaldehyde in PBS, pH 7.4, and kept in this fixative for 1.5 h at room temperature. Between every step, the cochlear samples were washed at least three time with PBS for 5–10 min each wash. After decalcification with 4% sodium EDTA solution (adjusted with HCl to pH 7.4) for 3 d at 4 °C, the cochleae were micro-dissected into three turns (apex, middle, and base) and adhered to 10-mm round coverslips (Microscopy Products for Science and Industry,#260367) with cell-Tak (BD Biosciences, #354240). The specimens were first permeabilized in 3% Triton X-100 solution and then blocked with 10% normal goat serum for 30 min each step at room temperature, followed by incubation with primary antibodies: rabbit monoclonal anti-cAMP (Abcam, #134901), mouse monoclonal anti-3-nitrotyrosine (3-NT) (Sigma-Aldrich, #N5538), rabbit polyclonal anti-4-hydroxynonenal (4-HNE) (Abcam, #46545), and rabbit monoclonal anti-p-AMPKα (Cell Signaling Technology, #2535) at 4 °C for 48 h. The specimens were then incubated with the Alexa-Fluor-594-conjugated secondary antibody at a concentration of 1:200 at 4 °C overnight and followed by incubation with Alexa-Fluor-488-phalloidin for 1 h at room temperature in darkness. Control incubations were routinely processed without primary antibody treatments.

For immunolabeling of IHC synapses, the specimens were incubated in darkness at 37 °C overnight with primary monoclonal mouse anti-CtBP2 IgG1 at 1:200 (BD Biosciences, #612044) and mouse anti-GluA2 IgG2a at 1:2,000 (Millipore, #MAB397) followed with the Alexa-Fluor-594 goat anti-mouse IgG1 and Alexa-Fluor-488 goat anti-mouse IgG2a (1:1,000) at 37 °C for 1 h in darkness and then the step of secondary antibody labeling was repeated based on previous reports [13,37]. For visualization of sensory hair cells, the specimens were incubated with primary antibody polyclonal rabbit anti-myosin VIIa at 1:200 in darkness at 4 °C overnight (Proteus Biosciences, #25–6790) followed by incubation with Alexa Fluor 350 secondary antibody at a concentration of 1:200 at 4 °C overnight in darkness. For hair cell counts, the specimens were stained with Alexa-Fluor-488-phalloidin for 1 h.

After at least three final washes with PBS, all immunolabeling samples (already on round coverslips) were mounted by adding 8 μL mounting agent (Fluoro-gel with Tris buffer, Electron Microscopy Sciences, #17985-10) and sandwiched with another round coverslip and placed on a microscope slide. Finally, edges were sealed with nail polish. Immunolabeled images were taken with a 63 × -magnification lens under identical Z-stack conditions using Zeiss LSM 880 [39]).

### 2.6. Semi-quantification of the immunolabeling signals from outer hair cells of surface preparations

Immunohistochemistry is well accepted as a semi-quantitative methodology when used with careful consideration of the utility and semi-quantitative nature of these assays [40,41]. The specificity of antibodies must be first detected by Western blot. Antibodies showing only a single band with the correct molecular weight were used for immunolabeling on surface preparations. The regions of interest were outlined within individual OHCs based on the counterstaining. The grayscale value was assessed in OHCs to quantify the changes. This procedure provided semi-quantitative measurements that are not confounded by protein expression in other cell types of the cochlea.

Immunolabeling for cAMP, 3-NT, 4-HNE, and p-AMPKα was semi-quantified from original confocal images with 8-bit grayscale values, each taken with a 63X-magnification lens under identical conditions and equal parameter settings for laser gains and photomultiplier tube (PMT) gains within linear ranges of the fluorescence, using Image J software (National Institutes of Health, Bethesda, MD, USA). The cochleae from the different groups were fixed and immunolabeled simultaneously with identical solutions and processed in parallel. All surface preparations were counterstained with Alexa Fluor 488 phalloidin (green) to identify the comparable parts of the OHCs in confocal

images. The regions of interest of individual OHCs were outlined with the circle tool based on phalloidin staining. The immunolabeling labeling in grayscale in OHCs was measured in the upper-basal region (corresponding to sensitivity to 22–32 kHz) of surface preparations in 0.12-mm segments, each containing about 60 OHCs. The intensity of the background was subtracted and the average grayscale intensity per cell was then calculated. For each repetition, the relative grayscale value was determined by normalizing the ratio to control. Since there were no significant changes in immunolabeling for cAMP, 3-NT, 4-HNE, or p-AMPKα in the apex and middle regions of cochlear OHCs when assessed 1 h after the completion of noise exposure, we performed only semi-quantification of the immunolabeling signals from OHCs at the basal turn.

### 2.7. Quantification of the immunolabeled ribbons from Z projections on surface preparations

We have followed a procedure as previously described [13]. The number of presynaptic ribbons labeled with CtBP2 on surface preparations was quantified from original confocal images, each taken with a 63 × -magnification lens under identical Z-stack conditions (in 0.25-μm Z-steps) and equal parameter settings for laser gains and PMT gains. The z-stack images in each 0.12-mm segment (containing about 16 IHCs) were captured from cochlear surface preparations. The number of synaptic ribbons was counted using ImageJ software (National Institutes of Health, Bethesda, MD). Briefly, the background of the images was subtracted, the noise was despeckled once, and the threshold was set to isolate the immunolabeling of ribbon signals. The image was then converted to a binary file and the number of ribbon particles was counted using the 3D Object Counter and divided by the total number of IHC nuclei within the image.

### 2.8. Hair cell counts

Images from the apex through the base of the Alexa-Fluor-488-phalloidin-stained preparations were captured using a 20 × lens on the Zeiss microscope. The lengths of the cochlear epithelia were measured and recorded in millimeters. OHCs were counted from the apex to the base along the entire length of the mouse cochlear epithelium. The percentage of hair cell loss in each 0.5-mm length of epithelium was plotted as a function of the cochlear length as a cytocochleogram [42].

Mapping of frequencies as a function of distance along the entire length of the cochlear spiral was calculated with the equation [d (%) = 156.5–82.5 x log (f)] from Müller's paper [43]. The results are in agreement with the literature [44].

### 2.9. Forskolin treatment and hydrogen peroxide exposure of HEI-OC1 cells

HEI-OC1, an inner ear cell line, was kindly provided by Dr. Federico Kalinec at UCLA Health. HEI-OC1 cells were seeded in 6-well dishes to about $2 \times 10^5$ cells/well and cultivated in Dulbecco's modified eagle's medium (DMEM, Invitrogen, #11965-084) containing 4.5 g/L glucose and 10% fetal bovine serum (FBS) (Fisher scientific, #16000044) in a humidified incubator (37 °C, 5% $CO_2$, 95% humidity). After 24 h, cells were grown to 70% confluency and were then treated with 100 μM forskolin for 12 h. The control group was treated with the same volume of DMSO. Then each group was treated with hydrogen peroxide at 10 mM (Thermo Fisher Scientific, AC426000250) for 15 min. The cells were digested with 0.25% trypsin. The collected cells were transferred to a 15-mL conical tube (Corning, #430052) and centrifuged at 500 × *g* for 5 min and washed with 1 mL of PBS (Invitrogen, #20012). After removing the PBS, total protein was extracted using radio-immunoprecipitation (RIPA) buffer (Sigma, #R0278) containing phosphatase inhibitor (Roche, #04906845001) following the provided instructions. Finally, the total protein was stored at -80 °C after quantification. In this study, the HEI-OC1 cells used were between 20–40 culture passages.

#### 2.9.1. Annexin V/PI assay

An FITC-Annexin V/PI Apoptosis Kit (BD Pharmingen, #556547) was used to assess the $H_2O_2$-induced apoptosis of HEI-OC1 in accordance with the manufacturer's instructions. Briefly, cells were incubated in 6-well plates with DMEM supplemented with 10% FBS medium. After pre-treatment with 100 μM forskolin or vehicle control (DMSO) for 12 h, cells were exposed to 10 mM of $H_2O_2$ for 15 min. Then the cells were gently suspended in binding buffer and incubated in the dark at room temperature for 15 min with 5 μL Annexin V-FITC (fluorescein isothiocyanate) and 5 μL PI (propidium iodide). The Annexin V-FITC- and PI-labeled cells were analyzed using a flow cytometer (BD Biosciences). Dot plots of PI on the x-axis against Annexin V-FITC on the y-axis were used to distinguish viable cells, which were negative for PI and Annexin V-FITC. Cells in the early stages of apoptosis were Annexin V-positive and PI-negative, while cells in late apoptosis or full necrosis showed Annexin V-FITC-positive and PI-positive staining.

### 2.10. Cell vitality assay

Cultured HEI-OC1 cells were seeded in each well of a 96-well plate in triplicate. After attachment, the cells were treated with gradient doses of $H_2O_2$, with or without pretreatment of gradient doses of forskolin. Then cells were incubated for 2 h with Cell Counting Kit 8 (CCK-8) reagent (100 μL/mL medium) (VITA scientific, # DJDB4000x). Absorbance was determined at 490 nm using a microplate reader (BioTek Instruments).

### 2.11. Western blot analysis

Protein samples (30 μg) were separated by SDS-PAGE. After electrophoresis, the proteins were transferred onto a nitrocellulose membrane (Pierce) and blocked with 5% solution of nonfat dry milk in PBS-0.1% Tween 20 (PBS-T). The membranes were incubated with anti-total AMPKα (Abcam #39644, 1:1,000), anti-p-AMPKα (1:1,000) at 4 °C overnight, and then washed three times (10 min each) with PBS-T buffer. Membranes were then incubated with the appropriate secondary antibody at a concentration of 1:2,500 for 1 h at room temperature. Following extensive washing of the membrane, the immunoblot bands were visualized by SuperSignal West Dura Extended Duration Substrate or Pierce® ECL Western Blotting Substrate (Thermo Scientific). GAPDH was used (Cell Signaling Tech., # 5174, 1:3,000) as a sample loading control.

Western blot bands were scanned by LI-COR Odyssey Fc imaging system and analyzed using Image J software. First, the background staining density for each band was subtracted from the band density. Next, the probing protein/GAPDH ratio was calculated from the band densities run on the same gel to normalize for differences in protein loading. Finally, the difference in the ratio of the control and experimental bands was tested for statistical significance. Four samples were used for each group in all Western-blotting experiments.

### 2.12. Statistical analyses

Data were analyzed using SYSTAT 8.0 and GraphPad 5.0 software for Windows. Biological sample sizes were determined based on the variability of measurements and the magnitude of the differences between groups, as well as experience from our previous studies, with stringent assessments of difference. Data of OHC loss along the length of the cochlear spiral and synapse loss were analyzed with one-way repeated measures analysis of variance (ANOVA) with post-hoc comparison using SYSTAT 8.0. The rest of the analyses were done using GraphPad 5.0. Differences with multiple comparisons were evaluated by one-way ANOVA with multiple comparisons. Differences for single-

pair comparisons were analyzed using two-tailed unpaired Student's *t*-tests. Data for relative ratios of single-pair comparisons were analyzed with one-sample *t*-tests. A $p$-value $< 0.05$ was considered statistically significant. Data are presented as means ± SD or SEM based on the sample size and variability within groups. Sample sizes are indicated for each figure.

## 3. Results

### 3.1. Animal model

Previous research by our laboratory characterized models of noise-induced auditory damage in 12-week-old CBA/J mice under various exposure conditions [36]. In this study, we first measured auditory threshold shifts at 8, 16, and 32 kHz in 8-week-old CBA/J mice after exposure to octave band noise (OBN) with a frequency spectrum from 8–16 kHz for 2 h at a series of intensities. Exposure to 96 dB SPL resulted in auditory threshold shifts at 16 and 32 kHz as measured at day 1 after the exposure. These auditory threshold shifts gradually recovered with time and completely returned to baseline levels at day 7 after the exposure, i.e. the exposure induced temporary threshold shifts (TTS) (Fig. 1A–C). Exposure to 98 dB SPL resulted in auditory threshold shifts, some of which recovered to baseline levels on day 7, while some persisted at day 14 after the exposure, indicating some permanent hearing loss (Fig. 1D–F). Increasing the noise intensity to 100 dB SPL resulted in permanent threshold shifts (PTS) in all mice at all three tested frequencies (Fig. 1G–I). Therefore, we selected the intensity of 100 dB SPL to assess our hypothesis because PTS trauma is known to induce ROS formation and activate AMPKα, leading to sensory hair cell death.

### 3.2. Noise-induced ROS formation and activation of AMPKα are inhibited by antioxidant treatment

Previously, we found that noise-induced activation of AMPKα (p-AMPKα, T172), as detected in OHCs by a rabbit monoclonal antibody, can be inhibited through the specific inhibitor compound C or with AMPKα RNA silencing, which also effectively alleviate OHC loss and ABR threshold shifts [13]. Furthermore, we showed that noise-induced activation of p-AMPKα (T172) and total AMPKα1 were seen only in cochlear sensory hair cells assessed 1 h after completion of noise exposure, although total AMPKα2 appeared in cochlear sensory hair cells and supporting cells. In this study, we focused on p-AMPKα activation and oxidative stress markers (4-HNE and 3-NT) to explore the relationship between oxidative stress and p-AMPKα activation after noise trauma. Accumulation of ROS in noise-induced OHC death was assessed through markers of lipid peroxidation and protein nitration with 4-HNE and 3-NT, respectively [45]. Based on others' and our own prior publications showing that treatment with NAC at 350 mg/kg attenuates NIHL [36], we treated mice with NAC and evaluated immunoreactivity of 4-HNE in the left ears of our mice and activation of p-AMPKα in right ears 1 h after completion of PTS noise exposure. Levels of immunolabeling for both 4-HNE and p-AMPKα (converted to grayscale) were decreased in OHCs (Fig. 2A–D, $*p < 0.05$, $**p < 0.01$, $***p < 0.001$). These results indicate that ROS is a factor in activation of AMPKα in OHCs under noise exposure.

### 3.3. Noise-induced ROS formation and activation of AMPKα are inhibited by forskolin treatment

Forskolin is a stimulator of cAMP, a second messenger that can also serve as antioxidant due to its ability to indirectly remove ROS [46–49]. We therefore assessed 3-NT and 4-HNE protein levels with immunolabeling on cochlear surface preparations 1 h after completion of

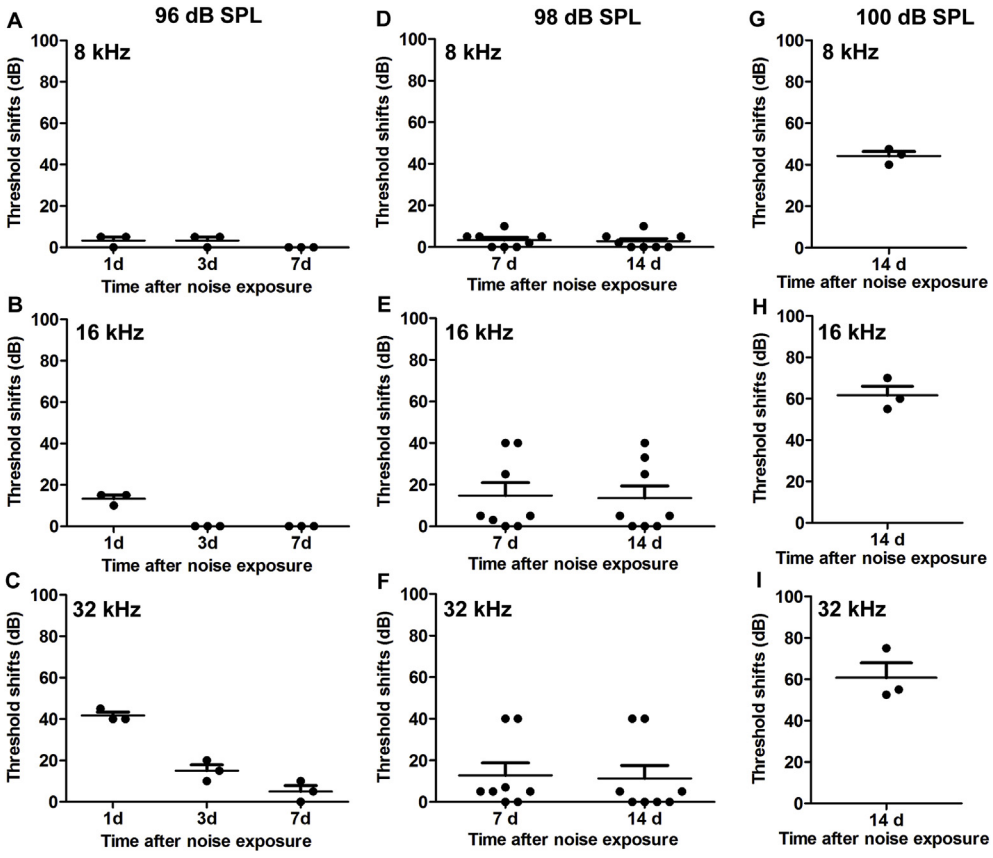


**Fig. 1. Noise-induced auditory threshold shifts for CBA/J mice at the age of 8 weeks.** (A–C) 96-dB SPL OBN exposure results in temporary auditory threshold shifts measured at 8, 16, and 32 kHz. Auditory threshold shifts were recovered 7 d after the exposure. (D–F) 98-dB SPL OBN exposure results in both TTS and PTS when measured by both 7 and 14 d after the exposure. (G–I) 100-dB SPL OBN exposure induces permanent threshold shifts when measured 14 d after noise exposure. Data are presented as individual points and means +SD.

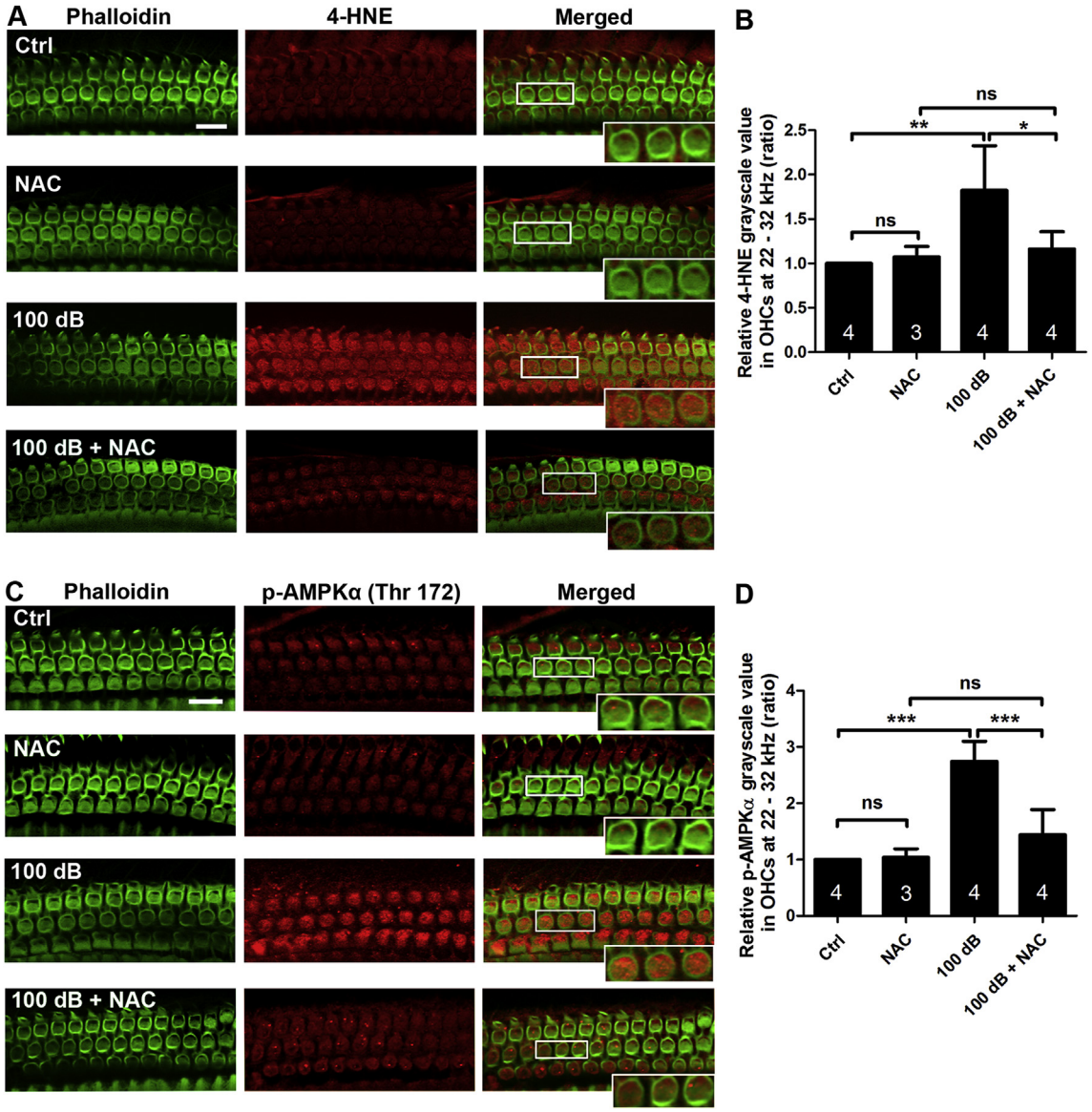


**Fig. 2. Treatment with antioxidant NAC reduces noise-induced 4-HNE and activation of AMPKα at T172.** (A–B) Assessment of 4-HNE in OHCs shows that NAC treatment significantly reduces noise-induced ROS accumulation in OHCs; NAC alone does not change ROS levels. (C–D) Activation of AMPKα triggered by noise exposure is significantly attenuated by treatment with NAC. Phalloidin (green) was used as counterstaining for visualization of OHCs; 4-HNE: 4-hydroxynonenal, Scale bar = 10 μm. Data are presented as means +SD. The number of animals in each group is indicated in the bar graph; one cochlea was used per mouse, ns: non-significant, $*p < 0.05$, $**p < 0.01$, $***p < 0.001$. (For interpretation of the references to colour in this figure legend, the reader is referred to the Web version of this article.)

the noise exposure, with or without concomitant forskolin treatment. In order to select a dose of forskolin, we probed the tolerance of mice to forskolin with administration of 5 mg/kg forskolin four times in 2 days via IP injections based on a report [50]. Fur appearance and body weight were unaffected by forskolin treatment. Our data were in agreement with the notion that noise exposure significantly increases the levels of ROS as marked by both 4-HNE and 3-NT in the OHCs (Fig. 3A, C, rectangular box, inset enlarged images from OHCs). After treatment with forskolin at 5 mg/kg for three doses, the noise-induced increases in 4-HNE and 3-NT in OHCs were completely blocked (Fig. 3A, C). Since loss of OHCs in the hook region was observed 1 h after the noise exposure and such loss follows a base-to-apex gradient, we selected quantification of 4-HNE- and 3-NT-immunolabeling in OHCs between 3.3–3.9 mm from the apex. This area corresponds to the region of sensitivity to 22–32 kHz. Semi-quantification of immunolabeling for 4-HNE and 3-NT in grayscale confirmed a significant increase by about 50% of both after the exposure. This noise-induced effect was completely blocked by forskolin treatment (Fig. 3B, D, $*p < 0.05$, $**p < 0.01$).

In agreement with the action of NAC, treatment with forskolin also significantly diminished noise-induced p-AMPKα at T172 in OHCs to near control levels (Fig. 4A and B), while treatment with forskolin alone did not influence the level of p-AMPKα. Furthermore, *in-vitro* experiments using HEI-OC1 cells also showed that use of 10 mM of $H_2O_2$ increased total levels of AMPKα ($p < 0.05$) and activation of AMPKα by densitometry analysis of total AMPKα and p-AMPKα (T172) bands on Western blots ($p < 0.05$, Fig. 5A–C). However, 100 μM forskolin inhibited this $H_2O_2$-induced activation of p-AMPKα (T172) ($p < 0.001$), but not total AMPKα (Fig. 5A–C). Additionally, administration of forskolin alone did not change the level of total AMPKα, but significantly reduced levels of p-AMPKα (T172) compared to the vehicle-alone group ($p < 0.05$) (Fig. 5A–C). All results support that ROS is a factor in activation of AMPKα in OHCs under noise exposure conditions.

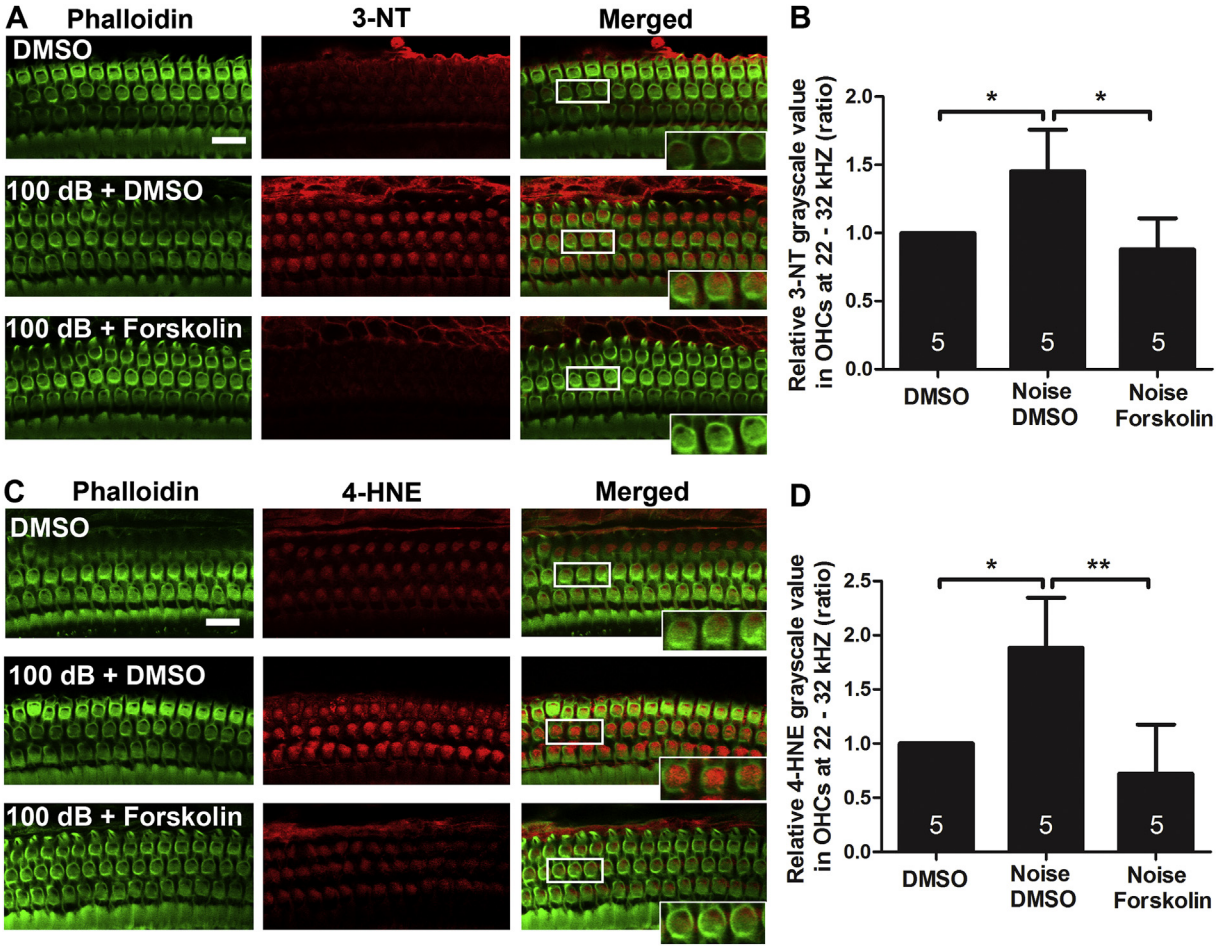


**Fig. 3. Treatment with forskolin alleviates noise-increased expression of 3-NT and 4-HNE levels in OHCs evaluated 1 h after completion of noise exposure.** (A and C) Treatment with forskolin prevented the noise-increased immunolabeling for 3-NT (red, A) and for 4-HNE (red, C) in OHCs. Representative images were taken from the upper basal turn. Phalloidin staining (green) illustrated OHC structure. 3-NT: 3-nitrotyrosine; 4-HNE: 4-hydroxynonenal, scale bar = 10 μm. (B and D) Semi-quantification of immunolabeling for 3-NT (B) and 4-HNE (D) in OHCs confirmed significant increase after noise exposure. These increases were inhibited by treatment with forskolin. Data are presented as means +SD. The number of animals in each group is indicated in the bar graph; one cochlea was used per mouse, $*p < 0.05$, $**p < 0.01$. (For interpretation of the references to colour in this figure legend, the reader is referred to the Web version of this article.)

### *3.4. Treatment with forskolin enhances cAMP levels in OHCs*

Since forskolin is a stimulator of cAMP, we immunolabeled cAMP on cochlear surface preparations to determine if forskolin treatment influences the levels of cAMP in OHCs. Treatment with forskolin alone significantly increased cAMP levels by 50% compared to the vehicle control (DMSO) group without noise exposure ($t_2 = 15.78$, $p = 0.004$). The level of immunoreactivity of cAMP in OHCs 1 h after the noise exposure were similar to age-matched controls without exposure; however, following treatment with forskolin, the level of cAMP in OHCs of the basal turn were increased by about 50% ($F_{3,\ 17} = 9.487$, $p < 0.05$) compared to noise-exposed DMSO-treated mice ($F_{3,\ 17} = 12.15$, $p < 0.01$, Fig. 6A and B). This result is in agreement with the notion that forskolin is a stimulator of cAMP.

### *3.5. Treatment with forskolin prevents noise-induced loss of outer hair cells and attenuates auditory threshold shifts*

Next, we tested the effects of forskolin against noise-induced hearing loss. There were no changes in auditory thresholds after forskolin-only or control injections with the vehicle DMSO (1 mL/kg DMSO) without noise exposure. Treatment with forskolin at 5 mg/kg for four doses via IP injections over 2 d alleviated noise-induced OHC loss by about 40% when assessed 14 d after the exposure. The loss of OHCs was significantly reduced at 2–5.5 mm from the apex along the cochlear duct (Fig. 7A and B, detailed statistical values listed in Table 2), but noise-induced IHC loss was not attenuated (Fig. 7C). In line with reduction of noise-induced OHC loss, treatment with forskolin also significantly attenuated noise-induced auditory threshold shifts measured at 8 kHz ($t_{14} = 4.876$, $p < 0.001$), 16 kHz ($t_{14} = 2.334$, $p < 0.05$), and 32 kHz ($t_{14} = 3.115$, $p < 0.01$) with an average reduction of threshold shifts of 32 dB, 17 dB, and 28 dB, respectively (Fig. 7D). These results demonstrate that treatment with forskolin prevents noise-induced loss of OHCs and PTS to some extent.

### *3.6. Treatment with forskolin did not prevent noise-induced loss of IHC ribbon synapses*

Since noise-induced reduction of IHC synapses has been well documented, we assessed if treatment with forskolin can attenuate loss of IHC synapses 14 d after the completion of noise exposure. Treatment with DMSO alone without noise exposure showed the number of synapses to be similar to the normal naïve group, as expected [13]. Additionally, our preliminary results did not show obvious disassociation of presynaptic ribbons immunolabeled with CtBP2 and postsynaptic terminals immunolabeled with GluA2 when assessed 2 weeks after noise exposure; we only counted the number of presynaptic ribbons immunolabeled with CtBP2. Based on our previous publication,

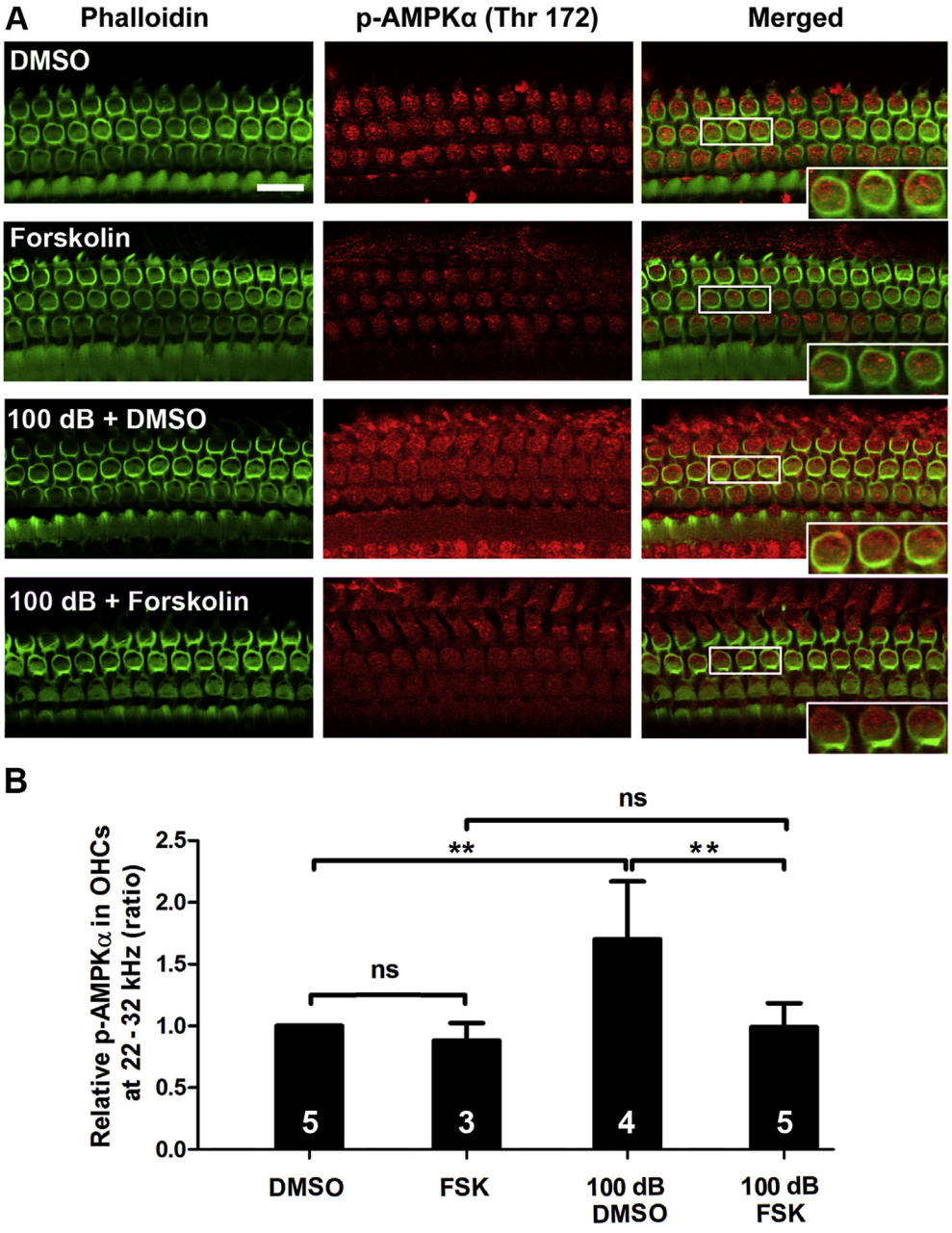


**Fig. 4. Treatment with forskolin reduces noise-increased p-AMPKα in OHCs examined 1 h after noise exposure.** (A) Treatment with forskolin prevented noise-increased immunolabeling for p-AMPKα (red) in OHCs. Phalloidin (green) was used as counterstaining for visualization of OHCs. Scale bar = 10 μm. (B) Quantification of immunolabeling for p-AMPKα in OHCs confirmed a significant increase after noise exposure, while treatment with forskolin prevented such noise effects. Data are presented as means +SD. The number of animals in each group is indicated in the bar graph; one cochlea was used per mouse, ns: non-significant, $^{**}p < 0.01$. (For interpretation of the references to colour in this figure legend, the reader is referred to the Web version of this article.)

broadband-noise-exposure-induced loss of synapses occurred only at higher frequencies (22 and 32 kHz) [13], whereas octave band noise -exposure-induced loss of synapses occurred in all of the five measured frequency regions (6, 8, 16, 22, and 32 kHz) [51]. Because mice were exposed to OBN in this study, we counted synaptic ribbons for these five frequency regions in three groups (DMSO alone, 100 dB + DMSO, and 100 dB + forskolin). OBN exposure significantly reduced the number of synaptic ribbons at all five analyzed frequencies as seen in the

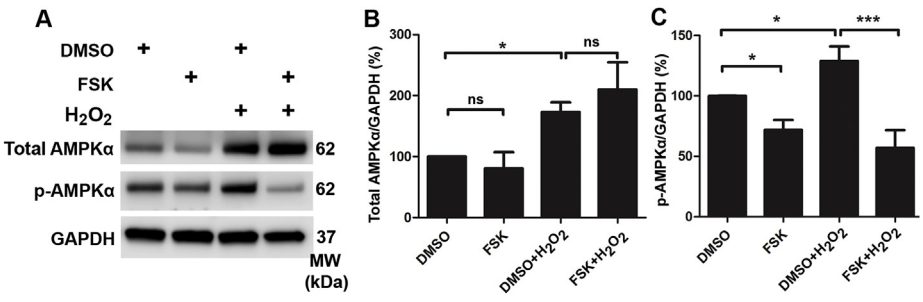


**Fig. 5. Administration of forskolin reduces $H_2O_2$-increased p-AMPKα levels in HEI-OC1 cells.** (A) Representative immunoblots show AMPKα and p-AMPKα with or without $H_2O_2$, forskolin, and vehicle control (DMSO) administration. HEI-OC1 cells were pre-treated with 100 μM forskolin for 12 h; the vehicle group was pre-treated with an equal concentration of DMSO. Then the groups were treated with 10 mM $H_2O_2$ for 15 min. GAPDH served as the sample-loading control. (B and C) Densitometry analysis of total AMPKα and p-AMPKα band densities normalized to GAPDH confirmed a significant increase in AMPKα and p-AMPKα by $H_2O_2$ administration. The activation on AMPKα by $H_2O_2$ was abolished by forskolin pre-treatment. Data (B and C) are presented as means +SD, $n = 4$ in each group, ns: no significant, $^{*}p < 0.05$, $^{***}p < 0.001$.

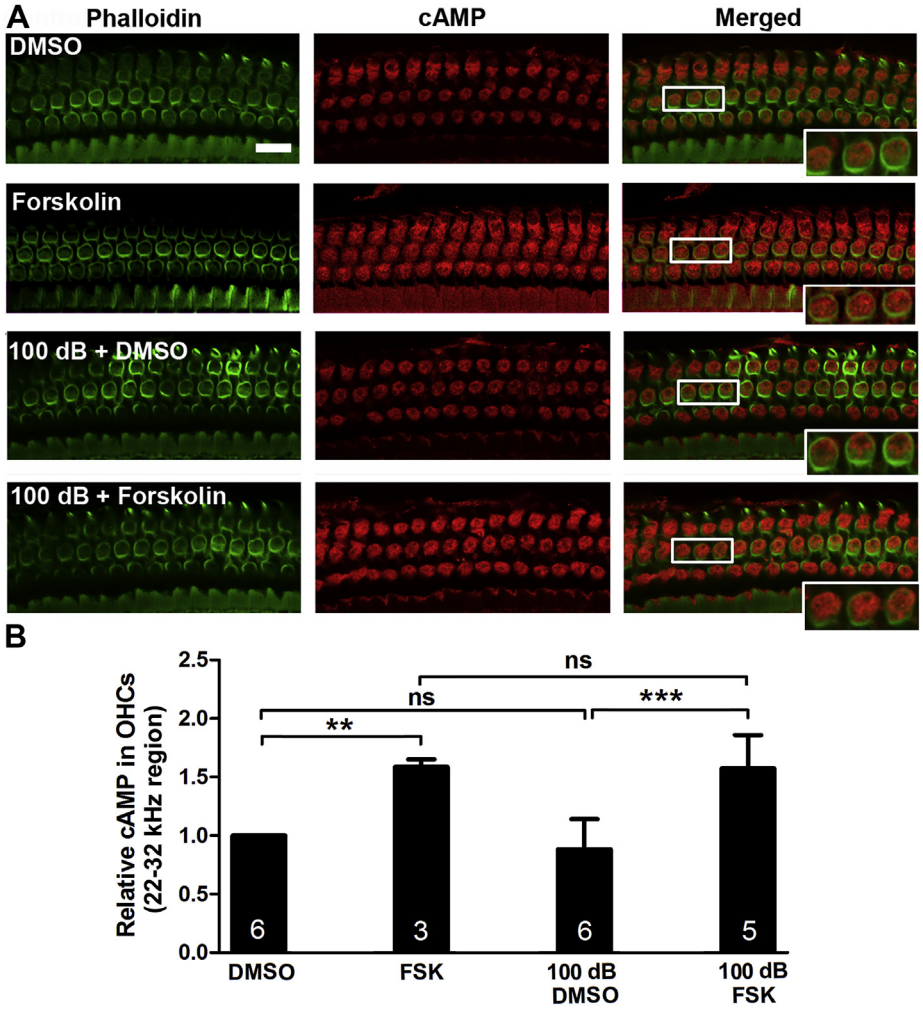


**Fig. 6. Noise exposure has no significant effect on cAMP levels in outer hair cells (OHCs), whereas treatment with forskolin increases cAMP expression in OHCs assessed 1 h after noise exposure.** (A) Representative images of immunolabeling for cAMP (red) in OHCs of surface preparations of the upper basal turn. Inset enlarged images are for visualization of labeling. Green: phalloidin, scale bar = 10 μm. (B) Semi-quantification of immunolabeling for cAMP in grayscale in OHCs revealed an increase after treatment with forskolin but not after noise exposure. Data are presented as means +SD. The number of animals in each group is indicated in the bar graph; one cochlea was used per mouse, ns: non-significant, $^{**}p < 0.01$, $^{***}p < 0.001$. (For interpretation of the references to colour in this figure legend, the reader is referred to the Web version of this article.)

comparison of the DMSO alone and 100 dB + DMSO groups, in agreement with our previous report using OBN exposure [51] (Fig. 8A and B, detailed statistical vales by repeated measure ANOVA analysis see Table 3, for detailed post-hoc test vales see Table 4). Co-treatment with forskolin did not attenuate noise-induced loss of synapses (Fig. 8A and B).

### 3.7. ROS-induced HEI-OC1 cell death is attenuated by forskolin treatment

The prevention of ROS-induced cell death after forskolin treatment is further confirmed by our *in-vitro* assays using HEI-OC1 cells with exposure to hydrogen peroxide ($H_2O_2$) for 15 min and employing a cell counting kit-8 (CCK-8) to detect cell viability. Treatment with doses of $H_2O_2$ ranging from 2.5–17.5 mM exhibited a dose-dependent decline in cell viability. Since forskolin was dissolved in 0.8% DMSO, we also evaluated treatment with 0.8% DMSO in HEI-OC1 cells for 12 h, which showed no effect on cell viability compared with the control group ($p > 0.05$). Pre-treatment with 100 μM forskolin for 12 h significantly improved cell viability after $H_2O_2$ application, when exposed to $H_2O_2$ at 7.5 mM ($t_7 = 5.956, p < 0.001$), 10 mM ($t_7 = 6.402, p < 0.001$) and 12.5 mM ($t_7 = 6.689, p < 0.001$). We further assessed a series of doses of forskolin against 10 mM $H_2O_2$ exposure. Administration of forskolin prevented the decrease in cell viability after $H_2O_2$ treatment in a dose-dependent manner, with forskolin doses ranging from 25–100 μM and with the most effective concentration being 100 μM ($p < 0.001$). Since CCK-8 analysis only assesses cell viability, we further analyzed the protective effect of 100 μM forskolin against $H_2O_2$-induced cell death by flow cytometry within four groups (DMSO vehicle alone, forskolin, DMSO + $H_2O_2$, and forskolin + $H_2O_2$) (Fig. 9A and B; $F_{12} = 39.21$, $p < 0.0001$). Treatment with 100 μM forskolin alone for 12 h has no cytotoxic effect on HEI-OC1 cells ($p > 0.05$), whereas exposure to 10 mM $H_2O_2$ for 15 min resulted in death of 24% of the HEI-OC1 cells ($p < 0.0001$). This $H_2O_2$ exposure-induced cell death was reduced by roughly half with pre-administration of 100 μM forskolin for 12 h ($p < 0.0001$) (Fig. 9A and B). We additionally analyzed the levels of $H_2O_2$-induced apoptotic ($F_{12} = 5.318$, $p = 0.0146$) and necrotic ($F_{12} = 37.49$, $p < 0.0001$) cell death separately (Fig. 9C and D). Both apoptotic (6%, $p < 0.05$) and necrotic HEI-OC1 cell death (18%, $p < 0.0001$) appeared after exposure to $H_2O_2$. This phenomenon is consistent with previous research using exposure of cells to $H_2O_2$ [52]. Pre-administration of 100 μM forskolin for 12 h prior to the $H_2O_2$ exposure significantly reduced necrotic-like cell death from 18% to 6% ($p < 0.0001$), but there was no reduction of apoptotic cell death (Fig. 9C and D). To some extent, the $H_2O_2$-induced HEI-OC1 cell death pattern, as a mix of necrosis and apoptosis, is similar as noise-induced OHC death [42]. These results offer further proof that treatment with forskolin has a protective effect against ROS damage.

## 4. Discussion

The salient results of this study are that noise-induced activation of AMPKα by phosphorylation at T172, detected by a rabbit monoclonal antibody in OHCs, is mediated at least in part by excessive ROS formation. Treatment with the antioxidant NAC or forskolin reduces noise-induced ROS formation, prevents activation of AMPKα, and thereby attenuates noise-induced losses of OHCs and NIHL.

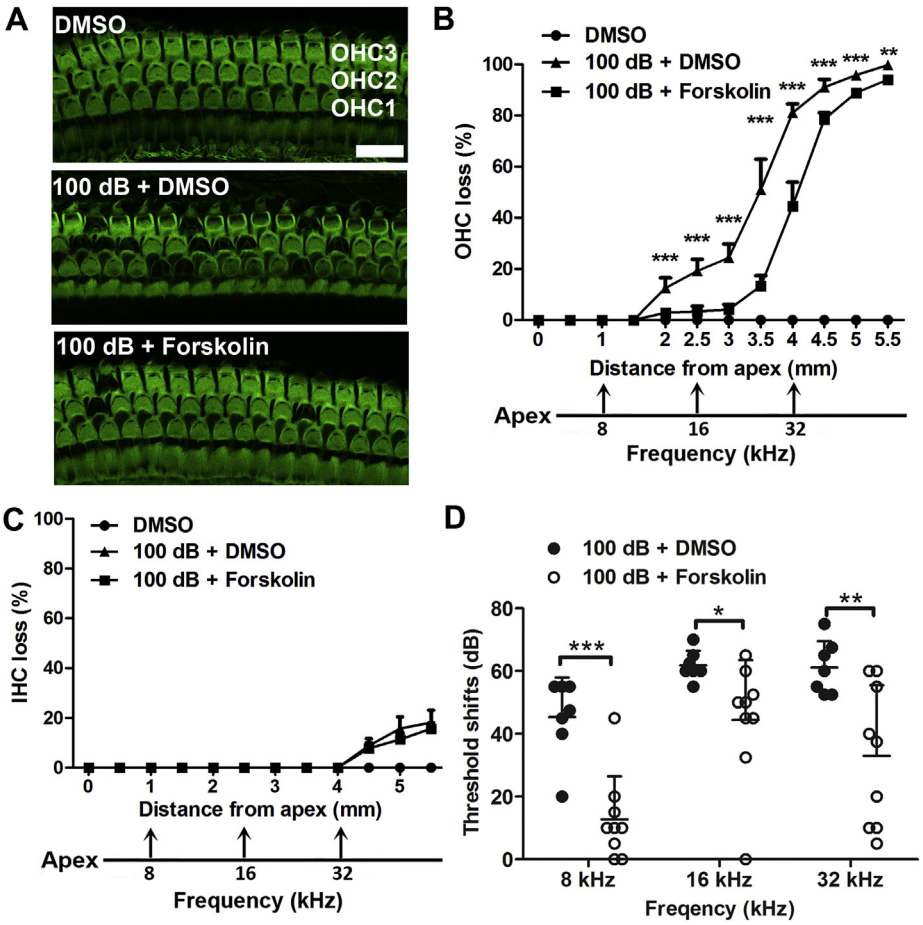


**Fig. 7. Treatment with forskolin attenuates noise-induced loss of outer hair cells and auditory threshold shifts 14 d after noise exposure.** (A) Representative images (corresponding to 3.5 mm from the apex of the cochlear spiral) display phalloidin-labeled sensory hair cells in the three groups of DMSO control, 100 dB + DMSO, and 100 dB + forskolin. OHC1, 2, and 3 indicate three rows of outer hair cells. Scale bar = 10 μm. (B and C) Treatment with forskolin reduces noise-induced OHC loss (B) but not IHC loss (C). Hair cells were counted along the entire length of the cochlear spiral. The distances along the cochlear duct that correlate with the frequencies of 8, 16, and 32 kHz are indicated. Data are presented as means +SEM, $n = 5$ in each group. (D) Noise-induced auditory threshold shifts were reduced by treatment with forskolin. Data are presented as individual point with means +SD; one cochlea was used per mouse, $^{*}p < 0.05$, $^{**}p < 0.01$, $^{***}p < 0.001$.

**Table 2**
Post-hoc analysis of OHC loss between 100 dB + DMSO vs 100 dB + Forskolin groups from the distance along the cochlear epithelia.

| Groups | Distance from apex (mm) | *p* value |
|---|---|---|
| 100 dB + DMSO vs 100 dB + Forskolin | 3.5 | $p < 0.0001$ |
| | 4 | $p < 0.0001$ |
| | 4.5 | $p < 0.0001$ |
| | 5 | $p < 0.0001$ |
| | 5.5 | $p = 0.003$ |

### *4.1. Numerous factors influence the susceptibility to NIHL and conditions of NIHL*

The susceptibility to NIHL in mouse models can be influenced by numerous factors including age, diet, circadian rhythms, the intensity of noise exposure, the strain of mouse, and animal care with or without use of dietary enrichments. In this study, exposure of 8-week-old CBA/J mice to 98 dB SPL noise results in auditory threshold shits with huge variations, as some mice show only TTS while others display PTS. However, exposure to 100 dB SPL for 2 h induces PTS with losses of both OHCs and IHCs in a fashion similar to that of exposure to 106 dB SPL in the same strain of mice at the age of 12 weeks [13,36,42]. Additionally, we were unable to induce PTS with loss of OHCs only (non IHC loss) when using 8-week-old CBA/J mice without dietary enrichments, although we have previously characterized such noise conditions with same strain mice at the age of 12 weeks [51,53]. Regardless of whether octave band (with a frequency spectrum from 8–16 kHz) or broadband noise exposure (with a frequency spectrum from 2–20 kHz) is used with mice at either age (8 or 12 weeks), noise-induced loss of sensory hair cells follows a base-to-apex gradient beginning in the basal turn [13,51,54]. In contrast, noise-induced loss of synapses differs between exposure to octave band and broadband noise in mice. With exposure to broadband noise, loss of synapses occurs only at higher frequencies (22 and 32 kHz) [13], whereas with exposure to octave band noise, loss of synapses appears at nearly all measured frequencies (8, 16, 22, and 32 kHz), but not at 5 kHz [51]. In line with this phenomenon, with exposure of 8-week-old mice to octave band noise in our current study, synapses loss appears at all measured frequencies (6, 8, 16, 22, and 32 kHz). This observation may related to the density of IHC synapses being laid out in a parabolic fashion along the length of the cochlear spiral with fewer synapses at the lowest and highest frequencies (beginning of the apical and end of the basal region of cochlear spiral), while the highest concentration of synapses centers on the 16 kHz region. Therefore, by exposure to octave band noise with a frequency spectrum from 8–16 kHz, a greater number of synapses in the regions from 6 to 32 kHz are reduced. Another possible reason may be the location of the L-type voltage-gated calcium channels (VGCC) that are the predominant VGCC in IHCs [55]. These channels are essential for presynaptic activity [56]. The over-activation of glutamate receptors on the postsynaptic terminals can cause excitotoxicity and swelling of the nerve terminals, resulting in anatomical and functional deficits.

### *4.2. Forskolin has antioxidant capacity and attenuates noise-induced loss of hair cells and NIHL*

In agreement with the notion that antioxidant treatment prevents NIHL [1], treatment with forskolin attenuates noise-induced loss of sensory hair cells and NIHL. Forskolin activates adenylyl cyclase [29] and treatment with forskolin increases cAMP levels in OHCs, while

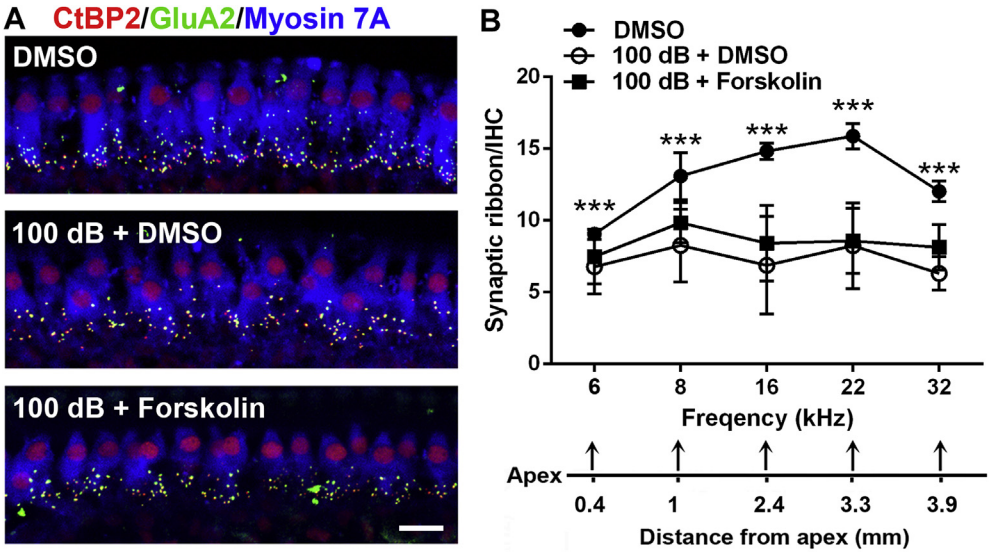


**Fig. 8. Treatment with forskolin does not attenuate noise-induced loss of inner hair cell synapses assessed 14 d after noise exposure.** (A) Representative images revealed immunolabeling for CtBP2 (red), GluA2 (green) and Myosin 7A. Images are comprised of Z-stack projections (in 0.25-μm Z-steps) taken from the area of the apical turn corresponding to 16 kHz, scale bar = 10 μm. (B) Quantification of CtBP2-immunolabeled ribbon particles in IHCs corresponding to 6, 8, 16, 22, and 32 kHz showed significant reduction at all frequencies after noise exposure. Treatment with forskolin showed no protective effect against noise-induced loss of synapses. The distances along the cochlear duct correlate with the frequencies as indicated. Data are presented as means ± SD, DMSO group: $n = 5$, 100 dB + DMSO: $n = 6$, 100 dB + Forskolin: $n = 6$, * indicates comparisons of DMSO group vs. 100 dB + DMSO, ***$p < 0.001$. (For interpretation of the references to colour in this figure legend, the reader is referred to the Web version of this article.)

**Table 3**
One-way ANOVA analysis of synapses between three groups at different frequencies.

| Groups | Frequency (kHz) | *F* value | *p value* |
|---|---|---|---|
| DMSO vs 100 dB + DMSO vs 100 dB + Forskolin | 6 | $F2,12 = 42.6$ | $p < 0.0001$ |
| | 8 | $F2,12 = 35.3$ | $p < 0.0001$ |
| | 16 | $F2,12 = 197.5$ | $p < 0.0001$ |
| | 22 | $F2,12 = 67.1$ | $p < 0.0001$ |
| | 32 | $F2,12 = 38.8$ | $p < 0.0001$ |

**Table 4**
Post-hoc analysis of synapses between DMSO group and 100 dB + DMSO group at different frequencies.

| Groups | Frequency (kHz) | *p* value |
|---|---|---|
| DMSO vs 100 dB + DMSO | 6 | $p < 0.0001$ |
| | 8 | $p < 0.0001$ |
| | 16 | $p < 0.0001$ |
| | 22 | $p < 0.0001$ |
| | 32 | $p < 0.0001$ |

noise exposure alone does not affect the levels of cAMP. As a second messenger, cAMP can be involved in regulation of cell survival pathways via protein kinase A (PKA) and CREB (cAMP response binding element) to produce antioxidants that counteract cellular ROS formation [57]. However, other studies show increased ROS after treatment with cAMP analogs [58]. With respect to these conflicting reports of whether cAMP increases or decreases ROS formation [59], our data demonstrate that treatment with forskolin diminishes noise-induced ROS in OHCs as assessed by oxidative markers 4-HNE and 3-NT in OHCs and attenuates NIHL, in line with a recent report showing that forskolin attenuates cisplatin-induced hearing loss [34]. However, the protective effect of forskolin varies widely between subjects with respect to auditory threshold shifts, especially at 32 kHz. Such variability may be due to the complexity of mechanisms of the different forms of cell death and progression of noise-induced OHC loss. Forskolin cannot address all possible ensuing pathways; as we previously reported, exposure of mice to 106 dB SPL induces both apoptotic and necrotic OHC death in mice at the age of 12 weeks [7,42]. Furthermore, such exposure resulting in permanent hearing loss with losses of both OHCs and IHCs is far more complicated to prevent than permanent hearing loss with loss of OHCs only [13,51].

Unfortunately, noise-induced loss of IHC synapses is not significantly prevented by forskolin treatment, which might be due to the severe noise trauma utilized in this study. This explanation is also in agreement with the notion that the integrity of the synapses is more vulnerable than OHCs to noise injury [60]. Treatment with antioxidant $CoQ_{10}$ attenuates noise-induced cortical dendritic injury [12], suggesting oxidative stress is involved in the mechanisms of noise-induced loss of IHC synapses. However, the noise conditions and species of animal used in our current study are different than the $CoQ_{10}$ study, making a direct comparison impossible.

### 4.3. Noise-induced activation of AMPKα is mediated by oxidative stress

Under traumatic noise exposure conditions, treatment with NAC attenuates noise-induced increases in ROS formation in OHCs, as measured by 4-HNE (in left ears) and activation of AMPKα in OHCs (using the right ears of the same mice), supporting the concept that activation of AMPKα is mediated by oxidative stress. Similar results also occur after forskolin treatment, reinforcing such a notion. In agreement with our *in-vivo* data, our *in-vitro* study using inner ear cell line HEI-OC1 cells, confirms activation of AMPKα at T172 with oxidative stress by direct administration of $H_2O_2$, strengthening the concept that ROS is a potential activator of AMPKα. Such a notion is in agreement with evidence that adding $H_2O_2$ to HEK-293 cells activates AMPK [26–28].

Our *in-vivo* study showing that treatment with forskolin attenuates noise-induced ROS formation, activation of AMPKα, and noise-induced OHC loss and NIHL indicates that, under pathological conditions of noise exposure, activation of AMPKα at T172 in OHCs leads to cell death. This notion is also supported by our *in-vitro* experiments showing that exposure of HEI-OC1 cells to $H_2O_2$ results in cell death that is prevented by forskolin treatment. However, activation of AMPK may initially upregulate antioxidant defenses by regulation of several antioxidant genes [61,62]. The dual effects of AMPK in the regulation of cell fate diverge depending on the duration of activation. Prolonged activation of AMPK results in the upregulation of pro-apoptotic proteins, such as BIM, in neurons [63]. Moreover, energetic stress can induce pro-apoptotic signals by AMPK through activation of p53 [64].

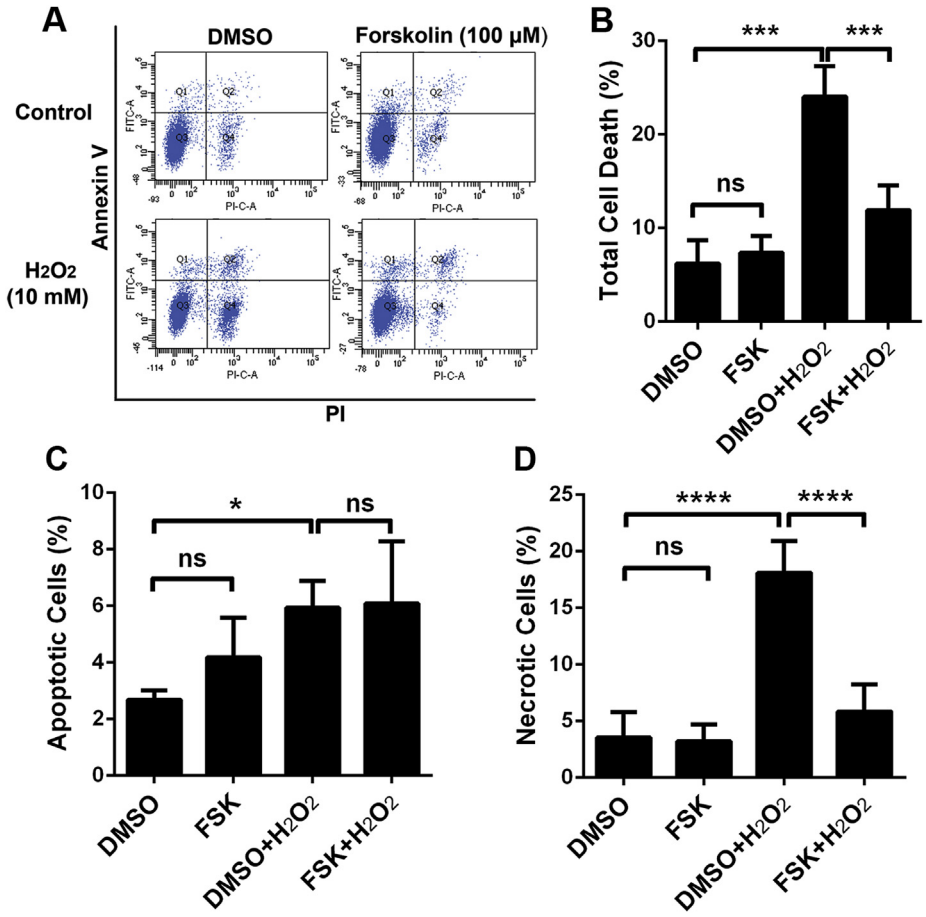


**Fig. 9. Administration of forskolin attenuates $H_2O_2$-induced HEI-OC1 cell death.** (A) An annexin V/PI flow cytometry assay shows that administration of $H_2O_2$ for 15 min with 10 mM resulted in approximately 25% HEI-OC1 cell death, whereas pre-treatment with forskolin (100 μM) for 12 h significantly reduced cell death. (B) Quantification of the percentage of total dead cells confirmed a significant difference. (C and D) revealed quantification of percentage of apoptotic (C) and necrotic (D) cell death, respectively. Data are presented as means +SD, $n = 4$, ns: non-significant, FSK: forskolin, $^{*}p < 0.05$, $^{***}p < 0.001$, $^{****}p < 0.0001$.

These contradictory effects of AMPK activation might be owed to its heterodimeric complex. In mammals, AMPK contains catalytic α-subunits and regulatory β- and r-subunits, with two isoforms of the α-subunit and three isoforms each of the β- and the r-subunits, resulting in 12 potential configurations of AMPK. Each variation of AMPK performs different functions under different physiological and pathological conditions [65]. Under excessive noise exposure (PTS noise conditions), transient intracellular ATP depletion is one of the initial responses in cochlear tissues in mice [54]. A potential pathway from transient ATP depletion to cell death involves the activation of AMPKα at T172. Further supporting this notion is the fact that silencing LKB, a protein kinase upstream of AMPKα, attenuates NIHL [13]. In fact, inhibition of AMPKα by siRNA to reduce noise-induced activity by about 30% in OHCs significantly reduces noise-induced hair cell loss and NIHL. Additionally, the AMPKα-specific inhibitor compound C effectively attenuates NIHL [13].

Since ROS is not the only trigger for AMPKα activation, other molecular events, such as calcium influx, may also mediate AMPKα activation. Noise-induced calcium ($Ca^{2+}$) influx in OHCs has been well-documented in the pathogenesis of NIHL. Our recent report shows that noise-exposure increases mitochondria calcium uniporter (MCU) in OHCs when evaluated 1 h after the noise exposure, indicating calcium overload in mitochondria [51]. The notion that calcium signaling can influence the cellular generation of ROS, from sources such as NADPH oxidases and mitochondria, has been well discussed in the recent literature [66,67]. Our results showing that suppressing ROS via treatment with antioxidants, such as NAC or forskolin, abolishes AMPKα activation when assessed 1 h after completion of noise exposure, suggest that ROS is central to molecular events under these noise exposure conditions. This expectation is in agreement with our previous report showing that ROS increases in OHCs when assessed 1 h after the completion of noise exposure [36] and is also in line with earlier studies showing that levels of ROS increase hours after noise exposure and persists for 7–10 d [45].

In summary, our results first address the link between noise-exposure-increased ROS formation, as indicated by enhancement of 4-HNE and 3-NT, and activated AMPKα in OHCs leading to hair cell death, suggesting that ROS is a potential activator of AMPKα in NIHL (Fig. 10). This notion is supported by the effects of treatment with NAC and forskolin in mice with noise exposure. Additionally, *in-vitro* exposure of an inner ear cell line of HEI-OC1 cells to $H_2O_2$ activates AMPKα, reinforcing this notion. Finally, attenuation of NIHL with forskolin reveals a possible protective agent against NIHL.

## Author disclosure statement

There are no conflicts of interest for any of the authors.

The data contained in the manuscript have not been previously published, have not been submitted elsewhere, and will not be submitted elsewhere while under review.

All research protocols were approved by the Institutional Animal Care & Use Committee at the Medical University of South Carolina. Animal care was under the supervision of Division of Laboratory Animal Resources at MUSC.

All authors have reviewed the contents of the manuscript, approve of its contents, and validate the accuracy of the data.

## Acknowledgements

The research project described was supported by grant R01 DC009222 from the National Institute on Deafness and Other Communication Disorders, National Institutes of Health, USA. This

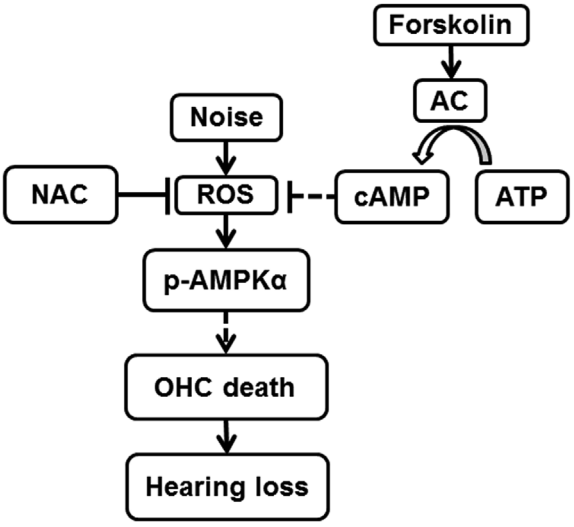


**Fig. 10.** The levels of ROS, indicated by products of lipid oxidation (4-HNE) and protein nitration (3-NT) in OHCs, increase after noise exposure. Such an increase activates p-AMPKα, leading to losses of ribbon synapses and OHCs, and NIHL. Treatment with forskolin, an adenylate cyclase (AC) activator, transforms ATP into cAMP in OHCs, which attenuates oxidative stress and activation of p-AMPKα.

work was conducted in the WR Building at MUSC in renovated space supported by grant C06 RR014516. Animals were housed in MUSC CRI animal facilities supported by grant C06 RR015455 from the Extramural Research Facilities Program of the National Center for Research Resources. We thank Dr. Jochen Schacht for his valuable comments on the manuscript. We also thank Andra Talaska for proof-reading of the manuscript.

## Appendix A. Supplementary data

Supplementary data to this article can be found online at https://doi.org/10.1016/j.redox.2019.101406.

## References

[1] S.H. Sha, J. Schacht, Emerging therapeutic interventions against noise-induced hearing loss, Expert Opin. Investig. Drugs 26 (2017) 85–96.
[2] H. Yamane, Y. Nakai, M. Takayama, H. Iguchi, T. Nakagawa, A. Kojima, Appearance of free radicals in the Guinea pig inner ear after noise-induced acoustic trauma, Eur. Arch. Oto-Rhino-Laryngol. 252 (1995) 504–508.
[3] W.J. Clerici, K. Hensley, D.L. DiMartino, D.A. Butterfield, Direct detection of ototoxicant-induced reactive oxygen species generation in cochlear explants, Hear. Res. 98 (1996) 116–124.
[4] K. Hirose, D.M. Hockenbery, E.W. Rubel, Reactive oxygen species in chick hair cells after gentamicin exposure in vitro, Hear. Res. 104 (1997) 1–14.
[5] K.K. Ohlemiller, J.S. Wright, L.L. Dugan, Early elevation of cochlear reactive oxygen species following noise exposure, Audiol. Neuro. Otol. 4 (1999) 229–236.
[6] H. Jiang, A.E. Talaska, J. Schacht, S.H. Sha, Oxidative imbalance in the aging inner ear, Neurobiol. Aging 28 (2007) 1605–1612.
[7] F.Q. Chen, H.W. Zheng, J. Schacht, S.H. Sha, Mitochondrial peroxiredoxin 3 regulates sensory cell survival in the cochlea, PLoS One 8 (2013) e61999.
[8] B.B. Song, S.H. Sha, J. Schacht, Iron chelators protect from aminoglycoside-induced cochleo- and vestibulo-toxicity, Free Radic. Biol. Med. 25 (1998) 189–195.
[9] S.H. Sha, J. Schacht, Antioxidants attenuate gentamicin-induced free radical formation in vitro and ototoxicity in vivo: D-methionine is a potential protectant, Hear. Res. 142 (2000) 34–40.
[10] S.H. Sha, J.H. Qiu, J. Schacht, Aspirin to prevent gentamicin-induced hearing loss, N. Engl. J. Med. 354 (2006) 1856–1857.
[11] D. Henderson, E.C. Bielefeld, K.C. Harris, B.H. Hu, The role of oxidative stress in noise-induced hearing loss, Ear Hear. 27 (2006) 1–19.
[12] A.R. Fetoni, P. De Bartolo, S.L. Eramo, R. Rolesi, F. Paciello, C. Bergamini, R. Fato, G. Paludetti, L. Petrosini, D. Troiani, Noise-induced hearing loss (NIHL) as a target of oxidative stress-mediated damage: cochlear and cortical responses after an increase in antioxidant defense, J. Neurosci. 33 (2013) 4011–4023.
[13] K. Hill, H. Yuan, X. Wang, S.H. Sha, Noise-induced loss of hair cells and cochlear synaptopathy are mediated by the activation of AMPK, J. Neurosci. 36 (2016) 7497–7510.
[14] S.A. Hawley, F.A. Ross, C. Chevtzoff, K.A. Green, A. Evans, S. Fogarty, M.C. Towler, L.J. Brown, O.A. Ogunbayo, A.M. Evans, D.G. Hardie, Use of cells expressing gamma subunit variants to identify diverse mechanisms of AMPK activation, Cell Metabol. 11 (2010) 554–565.
[15] D. Garcia, R.J. Shaw, AMPK: mechanisms of cellular energy sensing and restoration of metabolic balance, Mol. Cell 66 (2017) 789–800.
[16] S. Herzig, R.J. Shaw, AMPK: guardian of metabolism and mitochondrial homeostasis, Nat. Rev. Mol. Cell Biol. 19 (2018) 121–135.
[17] D.G. Hardie, Minireview: the AMP-activated protein kinase cascade: the key sensor of cellular energy status, Endocrinology 144 (2003) 5179–5183.
[18] D. Carling, F.V. Mayer, M.J. Sanders, S.J. Gamblin, AMP-activated protein kinase: nature's energy sensor, Nat. Chem. Biol. 7 (2011) 512–518.
[19] D.G. Hardie, D. Carling, S.J. Gamblin, AMP-activated protein kinase: also regulated by ADP? Trends Biochem. Sci. 36 (2011) 470–477.
[20] J.S. Oakhill, R. Steel, Z.P. Chen, J.W. Scott, N. Ling, S. Tam, B.E. Kemp, AMPK is a direct adenylate charge-regulated protein kinase, Science 332 (2011) 1433–1435.
[21] D.G. Hardie, F.A. Ross, S.A. Hawley, AMPK: a nutrient and energy sensor that maintains energy homeostasis, Nat. Rev. Mol. Cell Biol. 13 (2012) 251–262.
[22] S. Cardaci, G. Filomeni, M.R. Ciriolo, Redox implications of AMPK-mediated signal transduction beyond energetic clues, J. Cell Sci. 125 (2012) 2115–2125.
[23] S.M. Jeon, Regulation and function of AMPK in physiology and diseases, Exp. Mol. Med. 48 (2016) e245.
[24] E.C. Hinchy, A.V. Gruszczyk, R. Willows, N. Navaratnam, A.R. Hall, G. Bates, T.P. Bright, T. Krieg, D. Carling, M.P. Murphy, Mitochondria-derived ROS activate AMP-activated protein kinase (AMPK) indirectly, J. Biol. Chem. 293 (2018) 17208–17217.
[25] B.M. Emerling, F. Weinberg, C. Snyder, Z. Burgess, G.M. Mutlu, B. Viollet, G.R. Budinger, N.S. Chandel, Hypoxic activation of AMPK is dependent on mitochondrial ROS but independent of an increase in AMP/ATP ratio, Free Radic. Biol. Med. 46 (2009) 1386–1391.
[26] S.L. Choi, S.J. Kim, K.T. Lee, J. Kim, J. Mu, M.J. Birnbaum, S. Soo Kim, J. Ha, The regulation of AMP-activated protein kinase by H(2)O(2), Biochem. Biophys. Res. Commun. 287 (2001) 92–97.
[27] J.W. Zmijewski, S. Banerjee, H. Bae, A. Friggeri, E.R. Lazarowski, E. Abraham, Exposure to hydrogen peroxide induces oxidation and activation of AMP-activated protein kinase, J. Biol. Chem. 285 (2010) 33154–33164.
[28] F.R. Auciello, F.A. Ross, N. Ikematsu, D.G. Hardie, Oxidative stress activates AMPK in cultured cells primarily by increasing cellular AMP and/or ADP, FEBS Lett. 588 (2014) 3361–3366.
[29] R.H. Alasbahi, M.F. Melzig, Forskolin and derivatives as tools for studying the role of cAMP, Die Pharmazie 67 (2012) 5–13.
[30] M. Huerta, Z. Urzua, X. Trujillo, R. Gonzalez-Sanchez, B. Trujillo-Hernandez, Forskolin compared with beclomethasone for prevention of asthma attacks: a single-blind clinical trial, J. Int. Med. Res. 38 (2010) 661–668.
[31] R. Ouedraogo, X. Wu, S.Q. Xu, L. Fuchsel, H. Motoshima, K. Mahadev, K. Hough, R. Scalia, B.J. Goldstein, Adiponectin suppression of high-glucose-induced reactive oxygen species in vascular endothelial cells: evidence for involvement of a cAMP signaling pathway, Diabetes 55 (2006) 1840–1846.
[32] R. Palorini, D. De Rasmo, M. Gaviraghi, L. Sala Danna, A. Signorile, C. Cirulli, F. Chiaradonna, L. Alberghina, S. Papa, Oncogenic K-ras expression is associated with derangement of the cAMP/PKA pathway and forskolin-reversible alterations of mitochondrial dynamics and respiration, Oncogene 32 (2013) 352–362.
[33] Y.P. Zhang, Y. Zhang, Z.B. Xiao, Y.B. Zhang, J. Zhang, Z.Q. Li, Y.B. Zhu, CFTR prevents neuronal apoptosis following cerebral ischemia reperfusion via regulating mitochondrial oxidative stress, J. Mol. Med. (Berl.) 96 (2018) 611–620.
[34] X. Guo, X. Bai, L. Li, J. Li, H. Wang, Forskolin protects against cisplatin-induced ototoxicity by inhibiting apoptosis and ROS production, Biomed. Pharmacother. 99 (2018) 530–536.
[35] N.A. Malmquist, T.A. Moss, S. Mecheri, A. Scherf, M.J. Fuchter, Small-molecule histone methyltransferase inhibitors display rapid antimalarial activity against all blood stage forms in Plasmodium falciparum, Proc. Natl. Acad. Sci. U. S. A. 109 (2012) 16708–16713.
[36] H. Yuan, X. Wang, K. Hill, J. Chen, J. Lemasters, S.M. Yang, S.H. Sha, Autophagy attenuates noise-induced hearing loss by reducing oxidative stress, Antioxidants Redox Signal. 22 (2015) 1308–1324.
[37] G. Wan, M.E. Gomez-Casati, A.R. Gigliello, M.C. Liberman, G. Corfas, Neurotrophin-3 regulates ribbon synapse density in the cochlea and induces synapse regeneration after acoustic trauma, eLife 3 (2014).
[39] Q.-J. Fang, F. Wu, R. Chai, S.-H. Sha, Cochlear surface preparation in the adult mouse, J. Vis. Exp. (2019) e60299.
[40] C.R. Taylor, R.M. Levenson, Quantification of immunohistochemistry–issues concerning methods, utility and semiquantitative assessment II, Histopathology 49 (2006) 411–424.
[41] R.A. Walker, Quantification of immunohistochemistry–issues concerning methods, utility and semiquantitative assessment I, Histopathology 49 (2006) 406–410.
[42] H.W. Zheng, J. Chen, S.H. Sha, Receptor-interacting protein kinases modulate noise-induced sensory hair cell death, Cell Death Dis. 5 (2014) e1262.
[43] M. Muller, K. von Hunerbein, S. Hoidis, J.W. Smolders, A physiological place-frequency map of the cochlea in the CBA/J mouse, Hear. Res. 202 (2005) 63–73.
[44] A. Viberg, B. Canlon, The guide to plotting a cochleogram, Hear. Res. 197 (2004) 1–10.
[45] D. Yamashita, H.Y. Jiang, J. Schacht, J.M. Miller, Delayed production of free radicals following noise exposure, Brain Res. 1019 (2004) 201–209.
[46] A.G. Mahomed, A.J. Theron, R. Anderson, C. Feldman, Anti-oxidative effects of theophylline on human neutrophils involve cyclic nucleotides and protein kinase A, Inflammation 22 (1998) 545–557.

[47] H. Rakugi, N. Matsukawa, K. Ishikawa, J. Yang, M. Imai, M. Ikushima, Y. Maekawa, I. Kida, J. Miyazaki, T. Ogihara, Anti-oxidative effect of Klotho on endothelial cells through cAMP activation, Endocrine 31 (2007) 82–87.
[48] A. Bednarova, D. Kodrik, N. Krishnan, Adipokinetic hormone exerts its anti-oxidative effects using a conserved signal-transduction mechanism involving both PKC and cAMP by mobilizing extra- and intracellular Ca2+ stores, Comp. Biochem. Physiol.Toxicol.Pharmacol.CBICB (Curr. Biol.) 158 (2013) 142–149.
[49] J. Gu, L. Luo, Q. Wang, S. Yan, J. Lin, D. Li, B. Cao, H. Mei, B. Ying, L. Bin, F.G. Smith, S.W. Jin, Maresin 1 attenuates mitochondrial dysfunction through the ALX/cAMP/ROS pathway in the cecal ligation and puncture mouse model and sepsis patients, Lab. Investig. 98 (2018) 715–733.
[50] Y.T. Chiang, W. Ip, W. Shao, Z.E. Song, J. Chernoff, T. Jin, Activation of cAMP signaling attenuates impaired hepatic glucose disposal in aged male p21-activated protein kinase-1 knockout mice, Endocrinology 155 (2014) 2122–2132.
[51] X. Wang, Y. Zhu, H. Long, S. Pan, H. Xiong, Q. Fang, K. Hill, R. Lai, H. Yuan, S.H. Sha, Mitochondrial calcium transporters mediate sensitivity to noise-induced losses of hair cells and cochlear synapses, Front. Mol. Neurosci. 11 (2018) 469.
[52] K. Hayashi, K. Dan, F. Goto, N. Tshuchihashi, Y. Nomura, M. Fujioka, S. Kanzaki, K. Ogawa, The autophagy pathway maintained signaling crosstalk with the Keap1-Nrf2 system through p62 in auditory cells under oxidative stress, Cell. Signal. 27 (2015) 382–393.
[53] H. Xiong, H. Long, S. Pan, R. Lai, X. Wang, Y. Zhu, K. Hill, Q. Fang, Y. Zheng, S.H. Sha, Inhibition of histone methyltransferase G9a attenuates noise-induced cochlear synaptopathy and hearing loss, J Assoc Res Otolaryngol 20 (2019) 217–232.
[54] F.Q. Chen, H.W. Zheng, K. Hill, S.H. Sha, Traumatic noise activates Rho-family GTPases through transient cellular energy depletion, J. Neurosci. 32 (2012) 12421–12430.
[55] R. Fettiplace, Hair cell transduction, tuning, and synaptic transmission in the mammalian cochlea, Comp. Physiol. 7 (2017) 1197–1227.
[56] A. Brandt, J. Striessnig, T. Moser, CaV1.3 channels are essential for development and presynaptic activity of cochlear inner hair cells, J. Neurosci. 23 (2003) 10832–10840.
[57] A. Amaro-Ortiz, B. Yan, J.A. D'Orazio, Ultraviolet radiation, aging and the skin: prevention of damage by topical cAMP manipulation, Molecules 19 (2014) 6202–6219.
[58] P. Tai, M. Ascoli, Reactive oxygen species (ROS) play a critical role in the cAMP-induced activation of Ras and the phosphorylation of ERK1/2 in Leydig cells, Mol. Endocrinol. 25 (2011) 885–893.
[59] A. Dobi, S.B. Bravo, B. Veeren, B. Paradela-Dobarro, E. Alvarez, O. Meilhac, W. Viranaicken, P. Baret, A. Devin, P. Rondeau, Advanced glycation end-products disrupt human endothelial cells redox homeostasis: new insights into reactive oxygen species production, Free Radic. Res. 53 (2019) 150–169.
[60] S.G. Kujawa, M.C. Liberman, Adding insult to injury: cochlear nerve degeneration after "temporary" noise-induced hearing loss, J. Neurosci. 29 (2009) 14077–14085.
[61] D. Shao, S. Oka, T. Liu, P. Zhai, T. Ago, S. Sciarretta, H. Li, J. Sadoshima, A redox-dependent mechanism for regulation of AMPK activation by Thioredoxin1 during energy starvation, Cell Metabol. 19 (2014) 232–245.
[62] K. Zimmermann, J. Baldinger, B. Mayerhofer, A.G. Atanasov, V.M. Dirsch, E.H. Heiss, Activated AMPK boosts the Nrf2/HO-1 signaling axis–A role for the unfolded protein response, Free Radic. Biol. Med. 88 (2015) 417–426.
[63] C.G. Concannon, L.P. Tuffy, P. Weisova, H.P. Bonner, D. Davila, C. Bonner, M.C. Devocelle, A. Strasser, M.W. Ward, J.H. Prehn, AMP kinase-mediated activation of the BH3-only protein Bim couples energy depletion to stress-induced apoptosis, J. Cell Biol. 189 (2010) 83–94.
[64] R. Okoshi, T. Ozaki, H. Yamamoto, K. Ando, N. Koida, S. Ono, T. Koda, T. Kamijo, A. Nakagawara, H. Kizaki, Activation of AMP-activated protein kinase induces p53-dependent apoptotic cell death in response to energetic stress, J. Biol. Chem. 283 (2008) 3979–3987.
[65] B. Dasgupta, R.R. Chhipa, Evolving lessons on the complex role of AMPK in normal physiology and cancer, Trends Pharmacol. Sci. 37 (2016) 192–206.
[66] N. Hempel, M. Trebak, Crosstalk between calcium and reactive oxygen species signaling in cancer, Cell Calcium 63 (2017) 70–96.
[67] S. Feno, G. Butera, D. Vecellio Reane, R. Rizzuto, A. Raffaello, Crosstalk between calcium and ROS in pathophysiological conditions, Oxid. Med. Cell. Longev. 2019 (2019 Apr 24) 1–18 9324018.